A VARIATIONAL FINITE ELEMENT FORMULATION FOR THE TWO-DIMENSIONAL NAVIER-STOKES EQUATIONS

by

PETER A. GIESE

A thesis
presented to the University of Manitoba
in partial fulfillment of the
requirements for the degree of
MASTER OF SCIENCE
in
ELECTRICAL ENGINEERING

Winnipeg, Manitoba, 1984

A VARIATIONAL FINITE ELEMENT FORMULATION FOR THE TWO-DIMENSIONAL NAVIER-STOKES EQUATIONS

by

Peter A. Giese

A thesis submitted to the Faculty of Graduate Studies of the University of Manitoba in partial fulfillment of the requirements of the degree of

MASTER OF SCIENCE

ABSTRACT

A numerical method for the solution of the two-dimensional Navier-Stokes equations is developed using a variational finite element formulation in terms of the stream function and vorticity variables. A new approach to handling the no-slip condition is presented. The Newton-Raphson method is implemented as a means of solving the resulting nonlinear system of simultaneous equations. Numerical results are furnished to indicate the efficiency of the proposed method.

ACKNOWLEDGEMENTS

The author wishes to thank Dr. A. Wexler for his encouragement and guidance over the duration of this work. Dr. D. Trim and Dr. J. Shaw are thanked for many helpful discussions and suggestions.

The author thanks all his colleagues of the Computer-Aided Engineering and Numerical Applications Group for their invaluable assistance, especially Mr. R. Nakonechny and Mr. B. Klimpke.

CONTENTS

LIST OF FIGURES

Chapter I

INTRODUCTION

The numerical simulation of laminar fluid flow involves determining the unique solution of a set of partial differential equations under a given set of boundary conditions. Developing a general approach to solving the governing differential equations, most notably the Navier-Stokes equations, is an area of intense and on-going research.

The Navier-Stokes equations may be written for both turbulent and laminar flows. Turbulent flow is more difficult to simulate than laminar flow. There are unpredictable velocity fluctuations and complex viscosity interactions associated with turbulent flow [1, 2], which do not occur in laminar flows. The behavior of turbulent flow is still under investigation and to date no universal numerical calculation method exists. Turbulence simulation is not undertaken in this thesis.

What form the governing flow equations take depends not only on the type of flow being modeled, i.e. laminar or turbulent flow, but also on the variables being used to represent the flow. The Navier-Stokes equations can be expressed in terms of: the primitive variables velocity and

pressure; the stream function (ψ) and vorticity (ω); or by the stream function alone. In this study, the finite element method is applied to the stream function and vorticity formulation of the laminar, two-dimensional Navier-Stokes equations.

Chapter II presents the ψ and ω governing flow equations. The boundary conditions associated with each differential equation, including the no-slip boundary conditions, are reviewed. In addition, the pressure equation and the pressure boundary conditions are derived.

Three distinct approaches exist for the numerical solution of the laminar Navier-Stokes equations: 1) finite difference techniques; 2) finite element methods and; 3) boundary element methods. In the past, finite difference techniques played a prominent role in fluid dynamics but over the years this role has greatly diminished. Today's research is dominated by the finite element method [3]. The boundary element approach involves an integral formulation as a means of solving a differential equation [4, 5]. In fluid dynamics the boundary element method is not as well established as the finite element method, but it does hold promising prospects for the future.

The finite element solution of the Navier-Stokes equations is complicated by the nonlinearity of the system of equations and the necessity to include the no-slip condition. The most common techniques applied are methods

based on Galerkin formulations [6, 7], or penalty functions [8]. The method presented in this study departs from previous work in the following respects:

1. the finite element theory is based on a variational approach, utilizing a set of energy functionals; and
2. the no-slip boundary conditions are introduced directly without resorting to iterative schemes.

In the article [6], a direct method of introducing no-slip boundary conditions is formulated utilizing a set of constraint equations. The method being presented here makes use of the natural Neumann conditions associated with a variational formulation to introduce the no-slip boundary conditions. No additional constraint equations are required in the variational approach.

In Chapters III and IV the fundamental variational principles are presented and the finite element method is formulated. It is shown how the nonlinearity of the Navier-Stokes equations is treated. Using the properties of the energy functional, a direct method of enforcing the no-slip condition is derived. Other benefits arising from the variational finite element method are revealed.

The nonlinear system of simultaneous equations resulting from the finite element discretization process is solved iteratively using the Newton-Raphson method. The accuracy and convergence characteristics of the solution technique are demonstrated by way of examples which are presented in Chapter V.

Chapter II

GOVERNING FLOW EQUATIONS

The fundamental differential equations describing viscous fluid motion are the Navier-Stokes equations and the continuity equation [9]. In the derivation of the Navier-Stokes equations, the fluid is treated as a continuum under the assumptions that the fluid properties are isotropic and homogeneous.

The equations of motion can be simplified in the case of an incompressible, isothermal, laminar flow of a Newtonian fluid with no body forces. Under these restrictions the primary physical unknowns are reduced to velocity ($\overline{V}$) and pressure (P). Pressure is a scalar quantity whereas, in two-dimensions, velocity is a vector consisting of two components denoted as u and v.

It is a common practice in fluid dynamics to work with dimensionless quantities. In the case under consideration, the physical quantities used to produce the dimensionless groupings are: the free stream velocity U_0, a representative linear dimension L_0, as well as the fluid density ρ and the viscosity μ. The relationships between the dimensionless and primed dimensional quantities are:

$$u = \frac{u'}{U_0} , \qquad v = \frac{v'}{U_0} , \qquad P = \frac{P'}{\rho U_0^2} ,$$

$$x = \frac{x'}{L_0} , \qquad y = \frac{y'}{L_0} .$$

Under these constraints the dimensionless Navier-Stokes equations reduce to

$$u\frac{\partial u}{\partial x} + v\frac{\partial u}{\partial y} = -\frac{\partial P}{\partial x} + \frac{1}{Re}\nabla^2 u , \tag{2.1}$$

$$u\frac{\partial v}{\partial x} + v\frac{\partial v}{\partial y} = -\frac{\partial P}{\partial y} + \frac{1}{Re}\nabla^2 v , \tag{2.2}$$

and the continuity equation becomes

$$\frac{\partial u}{\partial x} + \frac{\partial v}{\partial y} = 0 . \tag{2.3}$$

The nature of incompressible flow, i.e. whether it is laminar or turbulent, is characterized by the Reynolds number. The Reynolds number is a dimensionless quantity defined as

$$Re = \frac{U_0 L_0 \rho}{\mu} = \frac{U_0 L_0}{\nu} ,$$

where ν is the kinematic viscosity. Dimensional analysis leads to the conclusion that for geometrically similar systems, the dynamic behavior of the flow depends only on the Reynolds number. The principle of similarity, first enunciated by O. Reynolds, is valid only if the forces

acting in the flow are due to friction and inertia. In the case of compressible fluids, or free surface flows, the problem is characterized by dimensionless quantities other than the Reynolds number.

Fluid motion is extremely dependent upon the geometry of the boundary surfaces as well as the actual surface properties. For a particular geometry the dynamical behavior of the fluid can be classified as laminar, transitional, or turbulent. The equations of motion, as stated above, are valid only for laminar flows. To analyze turbulent flow the Navier-Stokes equations must be modified to a time averaged form which includes spatially varying viscosity.

Care must be taken to ensure that a laminar Reynolds number is used and not a transitional or turbulent Reynolds number. Erroneously applying the laminar flow equations for turbulent flow will result in a mathematical field solution that would not have any physical significance.

2.1 STREAM FUNCTION AND VORTICITY FORMULATION

As an alternative to the velocity and pressure formulation it is possible to rewrite the governing equations in terms of the stream function and vorticity variables [10]. The stream function ψ is a scalar defined in terms of the velocity vector components

$$u = \frac{\partial \psi}{\partial y} , \qquad v = -\frac{\partial \psi}{\partial x} , \tag{2.4}$$

so that the continuity equation (2.3) is automatically satisfied. The vorticity vector is equal to the curl of the velocity vector. In two dimensions, the vorticity vector only has one component defined by

$$\omega = \frac{\partial v}{\partial x} - \frac{\partial u}{\partial y} \quad . \tag{2.5}$$

Because there is only one component, vorticity is treated as a scalar. Again, working with dimensionless quantities the following relationships occur:

$$\psi = \frac{\psi'}{U_0 L_0} , \qquad \omega = \frac{\omega' L_0}{U_0} \quad .$$

Differentiation of equations (2.1) and (2.2) with respect to y and x respectively, and elimination of pressure yields the steady vorticity transport equation. In terms of the dimensionless stream function and vorticity variables the equation reads

$$\nabla^2 \omega = Re\left[\frac{\partial \psi}{\partial y}\frac{\partial \omega}{\partial x} - \frac{\partial \psi}{\partial x}\frac{\partial \omega}{\partial y}\right] \quad . \tag{2.6}$$

Since there are two independent variables ψ and ω, but only one equation (2.6), a second differential equation is required. The second differential equation is obtained by introducing ψ into equation (2.5), which gives

$$\nabla^2 \psi = -\omega \quad . \tag{2.7}$$

The governing equations for steady, incompressible laminar flow in terms of the stream function and vorticity variables are equations (2.6) and (2.7). For a given Reynolds number, the ψ and ω solution is determined by solving the two governing flow equations simultaneously. Once the ψ solution is known the velocity field can be calculated through the definition of the stream function.

To obtain the pressure field a third equation is required. The pressure equation is derived by first differentiating equation (2.1) with respect to x and equation (2.2) with respect to y. The resulting equations are then added to give

$$-\nabla^2 P + \frac{1}{Re}\left[\frac{\partial}{\partial x}(\nabla^2 u) + \frac{\partial}{\partial y}(\nabla^2 v)\right] = \left(\frac{\partial u}{\partial x}\right)^2 + \left(\frac{\partial v}{\partial y}\right)^2 + 2\frac{\partial v}{\partial x}\frac{\partial u}{\partial y}$$

$$+ u\left[\frac{\partial^2 u}{\partial x^2} + \frac{\partial^2 v}{\partial x \partial y}\right] + v\left[\frac{\partial^2 u}{\partial x \partial y} + \frac{\partial^2 v}{\partial y^2}\right] \quad . \qquad (2.8)$$

Using the continuity equation (2.3), it can be shown that equation (2.8) reduces to

$$-\nabla^2 P = \left(\frac{\partial u}{\partial x}\right)^2 + \left(\frac{\partial v}{\partial y}\right)^2 + 2\frac{\partial v}{\partial x}\frac{\partial u}{\partial y} \quad .$$

Rearranging and introducing ψ into the above equation gives

$$\nabla^2 P = 2\left[\frac{\partial^2 \psi}{\partial x^2}\frac{\partial^2 \psi}{\partial y^2} - \left(\frac{\partial^2 \psi}{\partial x \partial y}\right)^2\right] \quad . \qquad (2.9)$$

Under the appropriate boundary conditions, the pressure field follows from the solution of equation (2.9) once ψ is known.

Individually each of the differential equations (2.6), (2.7) and (2.9) are linear, but because both ψ and ω appear in (2.6) and (2.7), together the two equations form a nonlinear system. The pressure equation (2.9) is the Poisson equation.

2.2 BOUNDARY CONDITIONS

Specifying the boundary conditions for a scalar field ϕ generally involves a Dirichlet or Neumann type boundary condition. The Dirichlet boundary condition

$$\phi(s) = g(s) \tag{2.10}$$

states the potential along the boundary. The boundary is denoted as s. The Neumann boundary condition

$$\left.\frac{\partial \phi}{\partial n}\right|_s = h(s) \tag{2.11}$$

defines the normal derivative of the field potential along the boundary. There is also a third type of boundary condition called the mixed.[1] The mixed condition does not occur in the type of problems discussed in this work.

The viscous fluid flow boundary conditions at a solid wall or surface correspond to the no-slip condition: both the normal and tangential velocity components are equal to zero. Rewriting the no-slip condition in terms of the stream function, it follows that both a constant Dirichlet and a

[1] The mixed condition is defined by $\partial\phi/\partial n + \alpha\phi(s) = k(s)$, where $k(s)$ is a given continuous function.

natural Neumann boundary condition must be enforced. Hence, the no-slip boundary conditions are:

$$\psi = c \ , \qquad \frac{\partial \psi}{\partial n} = 0 \ . \tag{2.12}$$

In general, no prior knowledge exists about the rate of change of velocity at a no-slip surface. Since vorticity is defined in terms of the derivatives of the velocity vector, nothing in general can be said about an ω boundary condition. On a no-slip boundary, ω remains an unknown and must be solved for explicitly.

Defining a pressure boundary condition requires knowing the velocity solution beforehand. A Neumann boundary condition is derived from the Navier-Stokes equations. In equation (2.1), substituting for ψ and transforming the Cartesian (x,y) coordinate system into normal (n) and tangential (τ) directions gives the Neumann boundary condition for pressure

$$\frac{\partial P}{\partial n} = \pm \frac{1}{Re}\left[\frac{\partial^3 \psi}{\partial \tau^3} + \frac{\partial^3 \psi}{\partial n^2 \partial \tau}\right] - \frac{\partial \psi}{\partial \tau}\frac{\partial^2 \psi}{\partial \tau \partial n} + \frac{\partial \psi}{\partial n}\frac{\partial^2 \psi}{\partial \tau^2} \ . \tag{2.13}$$

In accordance with the direction of the normal and tangential vectors, the sign will be either positive or negative. On a no-slip surface equation (2.1) can be simplified to

$$\frac{\partial P}{\partial x} = \frac{1}{Re}\left[\frac{\partial^2 u}{\partial x^2} + \frac{\partial^2 u}{\partial y^2}\right] \tag{2.14}$$

which, upon substitution of ψ, reduces to

$$\frac{\partial P}{\partial n} = \pm \frac{1}{Re} \frac{\partial^3 \psi}{\partial n^2 \partial \tau} \quad . \tag{2.15}$$

Alternatively, the no-slip Neumann condition can be stated in terms of ω rather than ψ [11]. From the continuity equation (2.3) the relationship

$$\frac{\partial^2 u}{\partial x^2} = - \frac{\partial^2 v}{\partial x \partial y}$$

is substituted into equation (2.14) to give

$$\frac{\partial P}{\partial x} = \frac{1}{Re} \frac{\partial \omega}{\partial y}$$

which reduces to

$$\frac{\partial P}{\partial n} = \pm \frac{1}{Re} \frac{\partial \omega}{\partial \tau} \quad . \tag{2.16}$$

Any combination of Dirichlet or Neumann boundary conditions can occur in a flow problem. Exactly what type of boundary conditions do occur depends on the velocity behavior of the fluid along the problem boundaries.

A further boundary condition is required for asymmetric flows. This usually takes the form of a Kutta condition or may be related to the Kelvin's theorem regarding the rate of shedding of vorticity. This boundary condition has not been imposed in the present work.

Chapter III

SOLUTION OF PARTIAL DIFFERENTIAL EQUATIONS BY FINITE ELEMENTS

As stated in Chapter II, the governing flow equations are partial differential equations. The next step is to find a means of solving the relevant differential equations.

Consider the operator equation $L\phi = f(x,y)$, where L is a differential operator which maps ϕ to f. Usually L and f are known and for a given set of boundary conditions we have the deterministic problem of finding ϕ, such that

$$\phi = L^{-1}f(x,y) \quad .$$

This is assuming that L^{-1} exists and the solution for ϕ is unique.

Except for a few special cases an analytical solution of the above form would prove to be very difficult. As an alternative to analytical methods, numerical solution techniques are considered. In this study we are concerned with a variational finite element method.

The flow equations can be arranged to take on the general form of the Poisson equation. The variational finite element method is first presented for the Poisson equation, then modified to include the Navier-Stokes equations.

3.1 VARIATIONAL PRINCIPLES

The variational approach involves minimization of a functional as a means of obtaining an energy convergent approximate solution to a partial differential equation. Not all differential operators possess the required properties that allow a variational formulation [12].

The variational method consists of formulating the partial differential equation of a field problem in terms of a variational expression called the energy functional. The appearance of the functional is dependent on both the differential operator and the applied definition of an inner product. A suitable inner product defined over the problem domain (Ω) is

$$\langle \phi_1, \phi_2 \rangle = \iint_{\Omega} \phi_1 \phi_2 \, dx \, dy \quad . \tag{3.1}$$

The inner product is valid for any admissible functions ϕ_1 and ϕ_2 which lie in the domain of the operator.[2] In the derivation of the functional the operator L is required to possess the following properties:

1. Linearity: $L[\alpha\phi_1 + \beta\phi_2] = \alpha L\phi_1 + \beta L\phi_2$
   for any scalars α and β.

---

[2] The problem domain is distinct from the domain of the operator. In two-dimensions the problem domain is an area. The domain of the differential operator consists of all continuous functions (with the exception of a finite number of discontinuities that have a finite norm) that satisfy the boundary conditions.

2. Self-Adjointness: $\langle L\phi_1, \phi_2 \rangle = \langle \phi_1, L\phi_2 \rangle$

3. Positive Definiteness: $\phi > 0, \ \langle L\phi, \phi \rangle > 0$

$\phi = 0, \ \langle L\phi, \phi \rangle = 0$

The minimal functional theorem [13, p.75] states that if L is a linear, self-adjoint and positive definite operator, the function ϕ which minimizes the functional

$$F(\phi) = \langle L\phi, \phi \rangle - 2\langle \phi, f \rangle \quad , \tag{3.2}$$

is also a solution of the equation

$$L\phi = f \quad , \tag{3.3}$$

under homogeneous boundary conditions. Referring to the operator properties, if L is self-adjoint the solution of equation (3.3) occurs at a stationary point of $F(\phi)$ and if L is positive definite, the stationary point corresponds to the minimum of $F(\phi)$.

The above functional is valid for a real vector space as opposed to the more general Hilbert space formulation [13, p.318]. To solve a differential equation under inhomogeneous boundary conditions the functional (3.2) must be modified.

3.2 FUNCTIONAL FORM FOR THE POISSON EQUATION

To define the energy functional for the Poisson equation

$$\nabla^2\phi = p(x,y)$$

a differential operator L must be specified. The operator can be either $L = -\nabla^2$ or $L = \nabla^2$. The former operator is positive definite whereas the latter is negative definite. The accepted convention is to work with a positive definite operator rather than a negative definite operator.

It can be shown that $L = -\nabla^2$ is a linear, self-adjoint and positive definite operator for the equation

$$-\nabla^2\phi = -p(x,y) = f(x,y) \quad . \tag{3.4}$$

Taking equation (3.1) and expanding equation (3.2) yields

$$F(\phi) = -\iint_\Omega \phi\nabla^2\phi \, dx \, dy - 2\iint_\Omega \phi f \, dx \, dy \quad . \tag{3.5}$$

Using the first form of Green's theorem

$$\iint_\Omega \nabla\phi\nabla\phi \, dx \, dy + \iint_\Omega \phi\nabla^2\phi \, dx \, dy = \int_s \phi\frac{\partial\phi}{\partial n} \, ds \quad ,$$

remembering that the functional (3.2) is valid under homogeneous boundary conditions gives

$$\iint_\Omega \nabla\phi\nabla\phi \, dx \, dy = -\iint_\Omega \phi\nabla^2\phi \, dx \, dy \quad .$$

Hence, it follows that

$$F(\phi) = \iint_\Omega (\nabla\phi\nabla\phi - 2\phi f) dx \, dy \quad . \tag{3.6}$$

In order to cater for inhomogeneous Neumann boundary conditions a new functional has to be derived. Fortunately, the functional for the Neumann problem is actually equation (3.6) with an additional boundary integral [13, 14]. The functional for inhomogeneous Neumann boundary conditions is

$$F(\phi) = \iint_{\Omega} (\nabla\phi\nabla\phi - 2\phi f)\, dx\, dy - 2\int_{S} \phi h\, ds \quad , \tag{3.7}$$

where h represents the Neumann condition (2.11).

A Dirichlet boundary condition does not alter the functional. Along a Dirichlet boundary ϕ is known and is not a variational parameter. It is understood that the trial functions used to approximate the solution ϕ must satisfy all of the Dirichlet boundary conditions. This makes equation (3.7) the general energy functional for the Poisson equation under both Dirichlet and Neumann boundary conditions. To determine the unique solution of equation (3.4) the minimum value of the functional (3.7) must be found.

3.3 FUNCTIONAL MINIMIZATION

Let the solution ϕ be approximated by ϕ_n, where ϕ_n represents a sum of linearly independent trial functions α_i with unknown coefficients ϕ_i

$$\phi_n = \sum_{i=1}^{m} \alpha_i \phi_i \quad . \tag{3.8}$$

The well known Rayleigh-Ritz method is a direct method of

functional minimization [15]. The Rayleigh-Ritz method determines the functional minimum by solving for the coefficient values ϕ_i that satisfy

$$\frac{\partial F(\phi_n)}{\partial \phi_i} = 0 \; ; \quad i = 1,2,3...m \; .$$

Once the coefficient values have been determined the approximate solution of equation (3.4) is known. If the operator is not only positive definite but as well positive-bounded-below, convergence of the functional to a minimum implies that the approximate solution approaches the exact solution in the mean.

Equation (3.8) can be conveniently expressed as

$$\phi_n = \underline{\alpha}^T \underline{\phi} = \underline{\phi}^T \underline{\alpha} \; , \tag{3.9}$$

where $\underline{\alpha}$ and $\underline{\phi}$ are column matrices. Substituting (3.9) into (3.7) yields

$$F(\phi_n) = \underline{\phi}^T \iint_\Omega \nabla\underline{\alpha} \nabla\underline{\alpha}^T \, dx \, dy \, \underline{\phi} - 2\underline{\phi}^T \iint_\Omega \underline{\alpha} f \, dx \, dy - 2\underline{\phi}^T \int_s \underline{\alpha} h \, ds \; .$$

Differentiating with respect to the variational parameters results in the expression

$$\frac{\partial F(\phi_n)}{\partial \underline{\phi}} = 2\iint_\Omega \nabla\underline{\alpha} \nabla\underline{\alpha}^T \, dx \, dy \, \underline{\phi} - 2\iint_\Omega \underline{\alpha} f \, dx \, dy - 2\int_s \underline{\alpha} h \, ds \; .$$

Setting the derivative equal to zero gives

$$\iint_\Omega \nabla\underline{\alpha} \nabla\underline{\alpha}^T \, dx \, dy \, \underline{\phi} = \iint_\Omega \underline{\alpha} f \, dx \, dy + \int_s \underline{\alpha} h \, ds \; . \tag{3.10}$$

Numerically evaluating the integrals in equation (3.10) and accumulating results in a linear system of simultaneous equations

$$S\underline{\phi} = \underline{b} \quad . \tag{3.11}$$

The minimum of the functional (3.7) is determined by solving equation (3.11) for the coefficients ϕ_i. It can be shown that the system matrix S is positive definite and symmetric.

Selecting a suitable set of α_i functions depends on the expected form of the field solution. For example, if the solution has field singularities then the trial functions should possess a singular term. Any set of trial functions may be selected, the only restriction being that they are linearly independent to ensure that the matrix S does not become singular.

3.4 FINITE ELEMENT DISCRETIZATION

The variational solution of the Poisson equation involves minimizing a functional, for a suitable set of trial functions. In this study isoparametric elements with quadratic serendipity polynomial shape functions are used to discretize the problem domain. In the local simplex the shape functions are:

$$\alpha_1 = \frac{1}{4}(1 - \xi)(1 - \eta)(-\xi - \eta - 1) \quad ,$$

$$\alpha_2 = \frac{1}{2}(1 - \xi^2)(1 - \eta) \quad ,$$

$$\alpha_3 = \frac{1}{4}(1 + \xi)(1 - \eta)(\xi - \eta - 1) \quad ,$$

$$\alpha_4 = \frac{1}{2}(1 + \xi)(1 - \eta^2) \quad ,$$

$$\alpha_5 = \frac{1}{4}(1 + \xi)(1 + \eta)(\xi + \eta - 1) \quad ,$$

$$\alpha_6 = \frac{1}{2}(1 - \xi^2)(1 + \eta) \quad ,$$

$$\alpha_7 = \frac{1}{4}(1 - \xi)(1 + \eta)(-\xi + \eta - 1) \quad ,$$

$$\alpha_8 = \frac{1}{2}(1 - \xi)(1 - \eta^2) \quad .$$

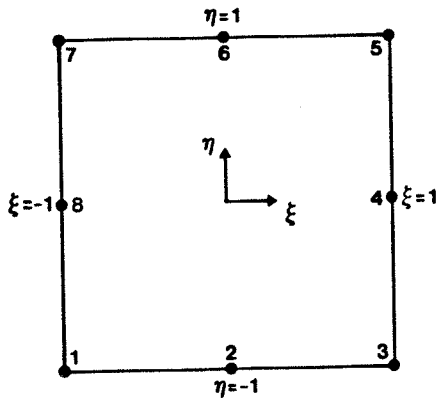

Figure 3.1: Local simplex.

The global positions in Cartesian coordinates are specified parametrically over each element by

$$x = \sum_{i=1}^{8} \alpha_i(\xi,\eta)x_i \qquad \text{and} \qquad y = \sum_{i=1}^{8} \alpha_i(\xi,\eta)y_i \quad ,$$

where x_i and y_i are the global node coordinates. The solution over each element is approximated by

$$\phi(x,y) = \sum_{i=1}^{8} \alpha_i(x,y)\phi_i \quad .$$

The problem domain is discretized into a finite number of quadrilateral elements, each uniquely represented by the above transformations. The serendipity shape functions enforce continuity of potential across adjacent element boundaries. For each element the functional (3.7) must be minimized such that the sum of all the functional values is also minimized [15].

Instead of evaluating the functional integrals in global space it is easier to perform the integrations in local space. By working in a local space the interval of integration remains unchanged regardless of what the interval of integration is in global space. The Jacobian of transformation, defined as

$$J = \begin{bmatrix} \frac{\partial x}{\partial \xi} & \frac{\partial y}{\partial \xi} \\ \frac{\partial x}{\partial \eta} & \frac{\partial y}{\partial \eta} \end{bmatrix} = \begin{bmatrix} \sum_{i=1}^{8} \frac{\partial \alpha_i}{\partial \xi} x_i & \sum_{i=1}^{8} \frac{\partial \alpha_i}{\partial \xi} y_i \\ \sum_{i=1}^{8} \frac{\partial \alpha_i}{\partial \eta} x_i & \sum_{i=1}^{8} \frac{\partial \alpha_i}{\partial \eta} y_i \end{bmatrix}$$

allows the region of integration to be modified. For instance, an area element in global space is transformed by

$$dx\,dy = \det[J]\,d\xi\,d\eta \quad .$$

The Jacobian matrix is also fundamental in the evaluation of derivatives in global space based on derivative values in local space.

A Gaussian quadrature numerical integration technique is used to approximate the values of each element integration. The accuracy of the Gaussian quadrature scheme depends on the order of quadrature: the higher the order the greater the accuracy [16]. A three point quadrature is used to evaluate all line integrals and a product form of the three point quadrature, which yields nine points, is used for all area integrals.

The functional (3.7) is applied whenever the Neumann boundary condition is encountered. If we assume the Neumann boundary condition is equal to zero, the boundary integral in equation (3.7) vanishes and we are left with the functional (3.6). The homogeneous Neumann boundary condition is automatically introduced if no boundary condition is specified. A homogeneous Neumann boundary condition occurs naturally, hence the name natural Neumann.

The system of simultaneous equations (3.11) is accumulated element by element. The values calculated for each element integration of equation (3.10) are stored in the S matrix according to the mesh node numbering scheme.

Along a Dirichlet boundary the functional (3.6) is applied. In accumulating the equation (3.11), a natural Neumann condition exists where the Dirichlet condition should be. To enforce the Dirichlet condition, a set of row and column permutations must be performed on the system matrix. Denoting $\phi_i^!$ as a Dirichlet node value, the manipulations consist of: 1) multiplying column i by $\phi_i^!$ and moving the result, with a change of sign, to the right-hand side; 2) deleting the row corresponding to $\phi_i^!$. Figure 3.2 illustrates the process of enforcing a Dirichlet boundary condition. Deleting the row corresponding to $\phi_i^!$ effectively removes the natural Neumann constraint and replaces it with the Dirichlet boundary condition. Once all permutations are performed, the resulting new set of simultaneous equations will include the appropriate Neumann and Dirichlet boundary conditions.

The finite element method using Lagrangian or serendipity shape functions possesses derivative discontinuities along adjacent element boundaries. As discussed in Section 3.3, one is not confined to using serendipity shape functions. The discontinuities caused by serendipity elements could be eliminated by utilizing higher order elements, such as Hermite or spline. While implementing higher order elements will quarantee derivative continuity across element boundaries, it is by far computationally more expensive and only moderately more accurate [17].

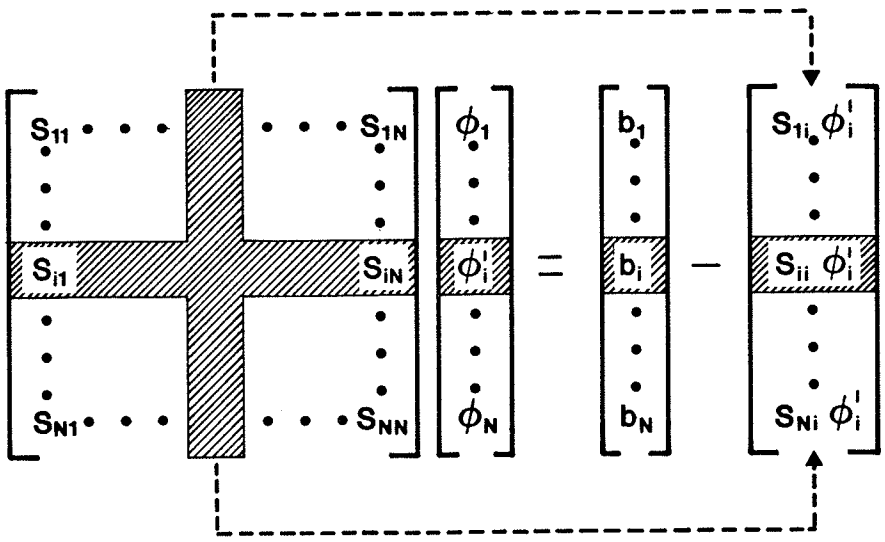

Figure 3.2: Dirichlet matrix permutations.

3.5 NEWTON-RAPHSON PRELIMINARIES

The solution of a linear system of equations can be accomplished in a direct manner, while the methods used in solving a nonlinear system of equations are iterative. The most frequently used iterative method for the solution of nonlinear finite element equations is the Newton-Raphson method [18, 19].

Expressing an arbitrary matrix system as

$$K\underline{\phi} = \underline{b}(\underline{\phi}) \quad ,$$

which, when written as a residual, becomes

$$\underline{R}(\underline{\phi}) = K\underline{\phi} - \underline{b}(\underline{\phi}) \quad . \tag{3.12}$$

An approximate solution for $\underline{\phi}$ is to be found such that $\underline{R}(\underline{\phi})=0$. Expanding equation (3.12) in the Taylor series and

retaining the first order terms gives

$$\underline{R}(\underline{\phi}^{N+1}) \equiv \underline{R}(\underline{\phi}^{N}) - \frac{\partial \underline{R}}{\partial \underline{\phi}}(\underline{\phi}^{N})\Delta\underline{\phi} \quad , \tag{3.13}$$

where

$$\underline{\phi}^{N+1} = \underline{\phi}^{N} - \Delta\underline{\phi} \quad . \tag{3.14}$$

By defining a Jacobian matrix as

$$J_{ij}^{N} = K_{ij} - \frac{\partial b_i(\phi^{N})}{\partial \phi_j} \quad ,$$

equation (3.13) can be rearranged into a linear set of equations defined by

$$J_{ij}^{N}\Delta\underline{\phi} = \underline{R}(\underline{\phi}^{N}) \quad . \tag{3.15}$$

Hence, the problem of solving a nonlinear system of equations has been reduced to an iterative sequence.

To determine the roots of equation (3.12) using the Newton-Raphson method, an initial estimate of $\underline{\phi}$ is chosen and $\Delta\underline{\phi}$ is determined from the system of simultaneous equations (3.15). The process of updating the $\underline{\phi}$ values followed by solving for $\Delta\underline{\phi}$ is repeated until the desired accuracy is obtained. This process will converge quadratically for a suitable starting estimate [20]. If the starting estimate is not in the vicinity of the solution the iterative process may diverge.

The Jacobian matrix that is generated at each intermediate step is sparse and nonsymmetric. Furthermore,

the topology of that matrix does not change as the iterative sequence proceeds.

Chapter IV

FINITE ELEMENT METHOD FORMULATION

The finite element method based on a variational principle reduces the problem of solving a partial differential equation to that of minimizing a certain functional. In this chapter the finite element methodology for the Poisson equation, already introduced in Chapter III, is expanded to include the governing flow equations

$$-\nabla^2\psi = \omega \quad , \tag{4.1}$$

$$-\nabla^2\omega = \mathrm{Re}\left[\frac{\partial\psi}{\partial x}\frac{\partial\omega}{\partial y} - \frac{\partial\psi}{\partial y}\frac{\partial\omega}{\partial x}\right] \quad . \tag{4.2}$$

The two independent variables ψ and ω are coupled through the interdependence of the differential equations. Initially the flow equations are viewed and treated as independent equations and not as coupled equations. For each differential equation, a functional is defined and a set of simultaneous equations is generated. The Newton-Raphson method combines the individual sets of simultaneous equations to form one large system of equations. Inherent within the combined system is the nonlinear interdependence of ψ and ω.

The problem domain is discretized using quadrilateral serendipity elements. Since there are two independent variables ψ and ω, one mesh is generated with two unknowns per node.

4.1 GENERATING THE SIMULTANEOUS EQUATIONS

In equation (4.1) ψ is treated as the unknown and ω is the source term. With ψ being the unknown the operator is the Laplacian. The functional for equation (4.1) takes on the same form as equation (3.7)

$$F(\psi) = \iint_{\Omega} (\nabla\psi\nabla\psi - 2\psi\omega)dx\, dy - 2\int_{s} \psi h\, ds \quad . \tag{4.3}$$

Minimizing the functional (4.3) over an element gives

$$\iint_{\Omega} \nabla\underline{\alpha}\nabla\underline{\alpha}^{T}\, dx\, dy\, \underline{\psi} = \iint_{\Omega} \underline{\alpha}\, \underline{\alpha}^{T}\, dx\, dy\, \underline{\omega} + \int_{s} \underline{\alpha} h\, ds \quad .$$

This yields a linear system of equations

$$S_{ij}\psi_j = b_{ij}\omega_j + C_i \quad . \tag{4.4}$$

When treating ω as the unknown, the operator for equation (4.2) is

$$L = -\nabla^2 - Re\, \frac{\partial\psi}{\partial x}\frac{\partial}{\partial y} + Re\, \frac{\partial\psi}{\partial y}\frac{\partial}{\partial x} \quad .$$

Before the minimal functional theorem can be applied it must be shown that this particular operator is linear, self-adjoint and positive definite. The operator is obviously

linear, but self-adjointness and positive definiteness of the operator cannot be shown because of the first derivatives. To overcome this problem, the right-hand side of equation (4.2) is transformed into a source term. The transformation process requires that the ω terms on the right-hand side be held as constants, independent of the ω terms on the left-hand side. The special notation of ω^* is used to emphasize this point

$$-\nabla^2\omega = \mathrm{Re}\left[\frac{\partial\psi}{\partial x}\frac{\partial\omega^*}{\partial y} - \frac{\partial\psi}{\partial y}\frac{\partial\omega^*}{\partial x}\right] \quad . \tag{4.5}$$

All the terms on the right-hand side of equation (4.5) can now be viewed as the source term in the Poisson equation and the operator becomes the Laplacian. The functional for equation (4.5) follows directly from the functional for the Poisson equation

$$F(\omega) = \iint_\Omega \nabla\omega\nabla\omega - 2\mathrm{Re}\omega\left(\frac{\partial\psi}{\partial x}\frac{\partial\omega^*}{\partial y} - \frac{\partial\psi}{\partial y}\frac{\partial\omega^*}{\partial x}\right) dx\, dy + 2\int_s \omega h\, ds \quad . \tag{4.6}$$

Minimizing this functional gives

$$\iint_\Omega \nabla\underline{\alpha}\nabla\underline{\alpha}^T dx\, dy\, \underline{\omega} = \mathrm{Re}\ \underline{\psi} \iint_\Omega \underline{\alpha}^T\left(\frac{\partial\underline{\alpha}}{\partial x}\frac{\partial\underline{\alpha}^T}{\partial y} - \frac{\partial\underline{\alpha}}{\partial y}\frac{\partial\underline{\alpha}^T}{\partial x}\right) dx\, dy\, \underline{\omega}^* + \int_s \underline{\alpha} h\, ds \quad .$$

The resulting system of equations, that minimizes the functional (4.6) over an element, takes on the form

$$S_{ij}\omega_j = \mathrm{Re}\psi_j D_{ijk}\omega_k^* + C_i \quad . \tag{4.7}$$

Within the integrand of each area integral there are

first derivative terms. The numerical Gaussian integration scheme reguires that these global first derivatives be evaluated at the Gauss points within each element. The process of evaluating the global derivatives based on the local derivatives involves the Jacobian of transformation. Global derivative evaluation is outlined in Appendix A.

One could attempt to solve for ψ and ω by iterating on ω: specify an initial guess for ω^*, solve equations (4.4) and (4.7) for ψ and ω, set ω^* equal to ω and repeat the process until convergence is obtained. In general, procedures based on the successive substitution of ω fail to provide satisfactory results. Past experiences of other researchers indicate that as the Reynolds number increases, the required number of iterations become exceedingly high [21]. There are no guarantees that an iterative method based on successive substitution will converge.

The variables ω and ω^* are treated as independent variables. This distinction enabled a functional for equation (4.2) to be derived and the corresponding system of simultaneous equations (4.7) to be generated. When viewed separately, equation (4.7) is valid for any set of ω^* values. However, when the two sets of simultaneous equation (4.4) and (4.7) are combined, and treated as a coupled system ω^* no longer remains arbitrary. There is only one unique set of ω^* values that permits the ψ and ω solution to have a physical meaning. The only meaningful solution arises

when ω^* is equal to ω. Therefore, the distinction between ω and ω^* is dropped from equation (4.7) to give

$$S_{ij}\omega_j = Re\psi_j D_{ijk}\omega_k + C_i \quad . \tag{4.8}$$

With two unknowns per node, the system matrix S_{ij} in equation (4.4) is identical to the system matrix in equation (4.8). In creating two functionals we have generated two sets of simultaneous equations, each of which minimizes a functional. A method that solves for ψ and ω satisfying equations (4.4) and (4.8), is required.

Because the problem is nonlinear, one can not solve both equations (4.4) and (4.8) simultaneously using a linear matrix inversion routine. To solve both sets of equations simultaneously the Newton-Raphson method is employed.

4.2 NEWTON-RAPHSON IMPLEMENTATION

The matrix equations (4.4) and (4.8) are coupled together and solved simultaneously by the Newton-Raphson method. Two residual vectors are defined; one corresponding to each system of equations

$$\begin{aligned} \underline{R}\,(\underline{\psi}) &= S_{ij}\psi_j - b_{ij}\omega_j = 0 \quad , \\ \underline{R}\,(\underline{\omega}) &= S_{ij}\omega_j - Re\ \psi_j D_{ijk}\omega_k = 0 \quad . \end{aligned} \tag{4.9}$$

As previously mentioned in Section 3.5 of Chapter III, the

iterative sequence

$$J^N_{ij}\underline{\Delta} = \underline{R}^N \quad , \tag{4.10}$$

is repeated until the exit criterion is satisfied. The Jacobian matrix is expressed in terms of the first derivatives of the residual vectors (4.9)

$$J^N_{ij} = \begin{bmatrix} \dfrac{\partial R_i(\underline{\psi})}{\partial \psi_j} & \dfrac{\partial R_i(\underline{\psi})}{\partial \omega_j} \\ \dfrac{\partial R_i(\underline{\omega})}{\partial \psi_j} & \dfrac{\partial R_i(\underline{\omega})}{\partial \omega_j} \end{bmatrix} \quad , \tag{4.11}$$

where

$$\frac{\partial R_i(\underline{\psi})}{\partial \psi_j} = S_{ij} \quad ,$$

$$\frac{\partial R_i(\underline{\psi})}{\partial \omega_j} = -b_{ij} \quad ,$$

$$\frac{\partial R_i(\underline{\omega})}{\partial \psi_j} = -\mathrm{Re}\, D_{ijk}\omega_k \quad ,$$

$$\frac{\partial R_i(\underline{\omega})}{\partial \omega_j} = S_{ij} - \mathrm{Re}\, \psi_k D_{ikj} \quad .$$

The $\underline{\Delta}$ vector in equation (4.10) is defined as

$$\underline{\Delta} = \begin{bmatrix} \Delta\psi_1 \\ \vdots \\ \Delta\psi_N \\ \Delta\omega_{N+1} \\ \vdots \\ \Delta\omega_{2N} \end{bmatrix} \quad . \tag{4.12}$$

The initial guess for ψ and ω was chosen to be zero. At each step in the iterative sequence the Jacobian matrix and the residual vectors are re-evaluated. The Newton-Raphson method solves the problem at hand by forming a sequence of linear approximations to the solution. The process is not always quaranteed to converge.

To determine if the process is converging or diverging, a suitable means of measuring convergence must be specified. Confronted with a variety of norms, each with different characteristics, it is rather difficult to recommend any one norm for all nonlinear analysis. A norm that is computationally easy to evaluate is the displacement norm. To gauge convergence, the displacement norm is taken as the ratio of the sum of all absolute values of $\underline{\Delta}$ to the sum of all absolute values of the previous node potentials. Typically, the exit criterion for such a norm would fall in the range 0.01 to 0.00001.

The two governing differential equations are coupled through the Jacobian matrix. The top half of the matrix corresponds to the set of simultaneous equations associated with equation (4.1), while the bottom half is directly associated with equation (4.2). The distinction between the two halves is fundamental in understanding the enforcement of the no-slip boundary conditions.

4.3 ENFORCING THE NO-SLIP BOUNDARY CONDITION

As discussed in Section 3.2 of Chapter III, the system of simultaneous equations resulting from the functional formulation is valid only under Neumann boundary conditions. A Dirichlet boundary condition is introduced by performing a set of column permutations and row eliminations on the system matrix. All Neumann and Dirichlet boundary conditions, except for the no-slip boundary conditions, are applied to the respective system of simultaneous equations (4.4) and (4.8) before being placed into the Jacobian matrix.

With two unknowns per node, there is an ω node value for every ψ value. Consider a node that lies on the no-slip boundary and denote the ψ and ω node variables as ψ^{I} and ω^{I}, respectively. In the process of accumulating equations (4.4) and (4.8) no ψ or ω boundary conditions are specified along a no-slip surface. As a consequence of not specifying a particular boundary condition, natural Neumann conditions on ψ^{I} and ω^{I} are introduced along the no-slip boundary. That is, for every ψ^{I} node there is a row in the top half of the Jacobian matrix which is associated with a ψ^{I} natural Neumann boundary condition. Also, in the bottom half of the Jacobian matrix, where ω^{I} occurs, there is a row associated with an ω^{I} natural Neumann boundary condition. In referring to a row of the Jacobian matrix (4.11), it is understood that the corresponding column entry in the residual vector of (4.12) is also being addressed.

The no-slip condition consists of a ψ constant Dirichlet and a ψ natural Neumann boundary condition, but no ω boundary condition exists. Modifications must be made to the Jacobian matrix in order to drop the ω natural Neumann condition and include the ψ constant Dirichlet boundary condition. To enforce both no-slip conditions a set of row and column permutations are performed on the Jacobian matrix (4.11).

The first step taken to enforce the no-slip condition is to delete the row associated with $\Delta\omega^1$ and move the row corresponding to $\Delta\psi^1$ into the vacated row. This step deletes the ω^1 natural Neumann condition and replaces it with the ψ^1 natural Neumann condition. Next, the constant Dirichlet boundary condition is enforced. In Section 3.4, the procedure for enforcing a Dirichlet condition was presented. The row and column operations that are performed to the set of equations (4.4) are converted to Jacobian row and column deletions. In the Jacobian matrix, the column associated with $\Delta\psi^1$ is deleted (the derivative of a constant equals zero) and the empty row associated with $\Delta\psi^1$ is also deleted.

The entire process of enforcing the no-slip boundary condition is graphically illustrated in Figure 4.1. Once the row and column operations are performed for all nodes that lie on the no-slip boundary, the Jacobian matrix can be inverted.

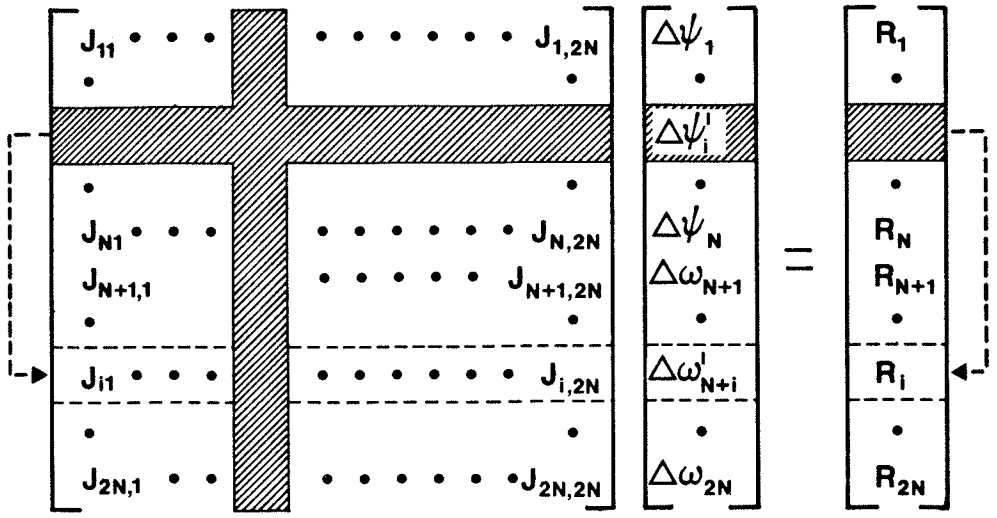

Figure 4.1: No-slip matrix permutations.

The no-slip condition requires that the entire no-slip surface be held at an equipotential. The above-mentioned procedure of enforcing the no-slip condition is only applicable when the constant Dirichlet value is known. In external flow problems, where the geometry of a no-slip surface is not symmetric, the constant ψ value is not known beforehand. When ψ is not known, an alternative method of enforcing an equipotential surface must be derived.

4.4 EQUIPOTENTIAL SURFACES

Although not implemented, the following is a brief description of a possible approach to enforcing an equipotential, no-slip surface. The proposed approach is a simple extension of the technique used to enforce the no-slip condition when ψ is known.

Depending on the finite element mesh, any number of nodes may lie on the no-slip surface. Consider two nodes ψ_i' and ψ_ℓ' that lie on the no-slip surface. To satisfy the constant Dirichlet condition we require that

$$\psi_i' = \psi_\ell' \quad . \tag{4.13}$$

This constraint is easily imposed upon the Jacobian matrix.

Just as before, the individual sets of matrix equations (4.4) and (4.8) are accumulated without specifying ψ or ω no-slip boundary conditions. The rows in the top half of the Jacobian matrix associated with $\Delta\psi_i'$ and $\Delta\psi_\ell'$ are moved to the bottom of the matrix to replace the rows corresponding to $\Delta\omega_{N+i}'$ and $\Delta\omega_{N+\ell}'$. The next step involves enforcing the equipotential condition. It can be verified that by simply adding the two columns associated with $\Delta\psi_i'$ and $\Delta\psi_\ell'$, and deleting one of the two empty $\Delta\omega'$ rows is equivalent to enforcing equation (4.13). Either row may be deleted, but only one row can be deleted. Performing the column addition and row deletion reduces the number of unknowns by one. The procedure is illustrated in Figure (4.2), note that the row corresponding to $\Delta\psi_\ell'$ is deleted and the row corresponding to $\Delta\psi_i'$ remains empty.

Regardless of how many nodes are involved, the process of accumulating rows and columns to enforce an equipotential condition will result in an under-determined system of equations. There is an empty row within the Jacobian

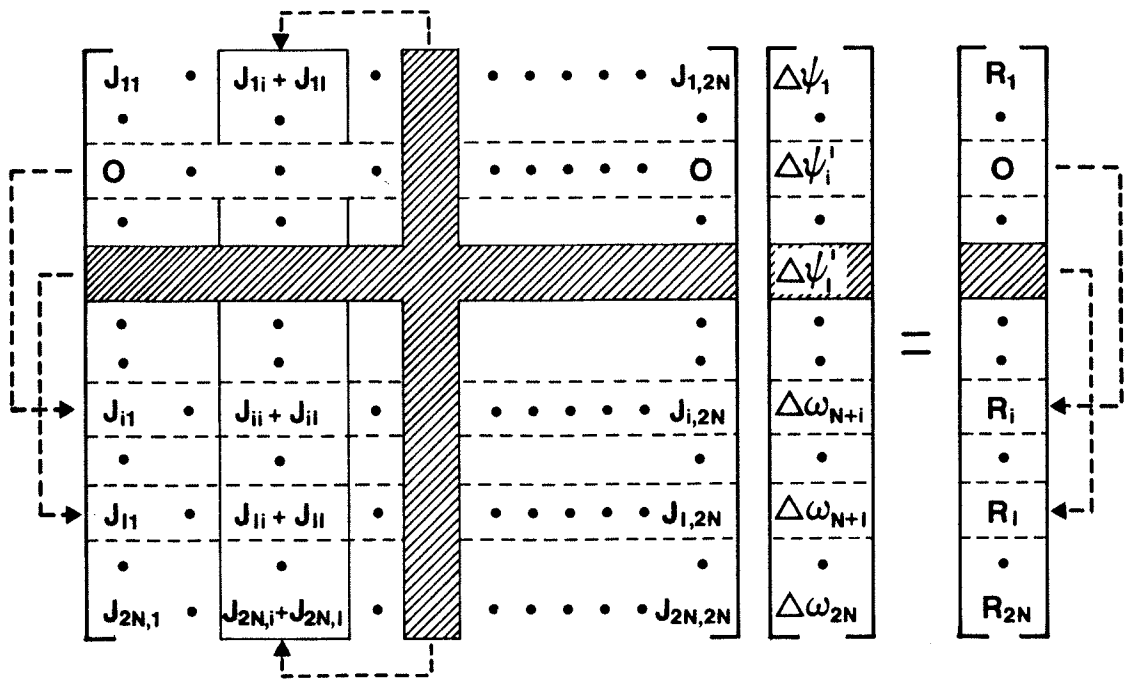

Figure 4.2: Equipotential surface matrix permutations.

matrix. An additional equation, linearly independent of all other equations, is required to complete the system.

Additional field constraints do exist. For example, in aerodynamics one can derive integral boundary conditions that follow from Kelvin's theorem and the related Kutta condition [22, 23]. However, it is not immediately clear how these conditions can be extended to include a multitude of no-slip surfaces in a simply connected configuration, nor is it obvious that a suitable constraint can be found in all conceivable cases. Finding a suitable constraint or boundary condition becomes problem dependent.

The proposed method does introduce both no-slip boundary conditions, but it remains to be determined how applicable the method is for solving equipotential problems. More research is required before the question of enforcing the no-slip condition for unknown ψ is fully answered.

4.5 SOLVING FOR THE STREAM FUNCTION AND VORTICITY

The ψ and ω solution is acquired variationally, despite the nonlinearity of the problem. The two ψ no-slip boundary conditions are introduced directly into the Jacobian matrix (4.11). The technique used to introduce the no-slip boundary conditions is a result of formulating the problem in terms of two energy functionals.

At each step of the Newton-Raphson algorithm equation (4.10) is generated and solved. Figure 4.3 shows the topology of a typical Jacobian matrix where each dot represents a nonzero entry. This matrix originates from the circular cylinder example presented in Section 5.1 of Chapter V.

Evident in Figure 4.3 is the symmetric nature of the Jacobian matrix. The topology of the matrix does not change with each iteration, but the individual matrix entries do. The Jacobian matrix is sparsely populated and nonsymmetric. All guarantees of strict diagonal dominance within the Jacobian matrix are lost by performing the no-slip row and column permutations. In fact, a zero entry may even occur on the diagonal.

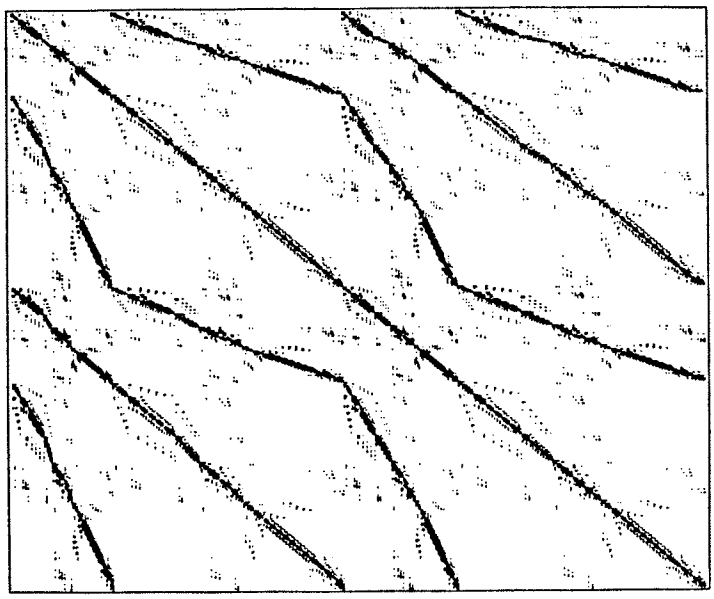

Figure 4.3: Jacobian sparsity pattern (527 unknowns).

The method used to solve the linear system of equations (4.10) is a partial pivoting Crout algorithm. The Crout algorithm is a direct method for solving a linear system of equations [24]. The Crout algorithm used in this study is an IMSL [25] routine that performs Gaussian elimination (Crout algorithm) with equilibration and partial pivoting. The IMSL version does not possess a sparsity storage scheme: the Jacobian is treated as a dense matrix. This particular version of the Crout algorithm was implemented because of its availability and general programming characteristics.

The terms on the right-hand side of equation (4.2) are all multiplied by the Reynolds number. Increasing the Reynolds number increases the nonlinearity of the problem.

The greater the nonlinearity, the more difficult it becomes for the Newton-Raphson algorithm to solve the problem. When the Reynolds number is too high, the simple starting estimate of zero everywhere may cause the iterative process to become unstable and diverge. Rather than trying to obtain a better starting estimate, it is much more practical to reduce the Reynolds number. The field solution at a reduced Reynolds number is then used as a starting estimate, enabling higher Reynolds number solution to be achieved.

Once the ψ and ω node values have been calculated to the desired accuracy, the velocity field and the pressure field can be determined. The velocity field follows directly from the definition of the stream function, whereas the pressure field involves solving the differential pressure equation.

4.6 THE PRESSURE SOLUTION

The finite element mesh used to discretize the ψ and ω fields is also used to discretize the pressure field. The functional for the pressure equation (2.9)

$$-\nabla^2 P = 2\left[\left(\frac{\partial^2\psi}{\partial x\partial y}\right)^2 - \frac{\partial^2\psi}{\partial x^2}\frac{\partial^2\psi}{\partial y^2}\right] \qquad (4.14)$$

is

$$F(P) = \iint_\Omega \nabla P\nabla P - 2P\left[\left(\frac{\partial^2\psi}{\partial x\partial y}\right)^2 - \frac{\partial^2\psi}{\partial x^2}\frac{\partial^2\psi}{\partial y^2}\right] dx\, dy + 2\int_s Ph\, ds \quad . \qquad (4.15)$$

The functional (4.15) is minimized

$$\iint_{\Omega} \nabla\underline{\alpha}\nabla\underline{\alpha}^{T}\, dx\, dy\, \underline{P} = \iint_{\Omega} \underline{\alpha}\left(\left(\frac{\partial^2\psi}{\partial x\partial y}\right)^2 - \frac{\partial^2\psi}{\partial x^2}\frac{\partial^2\psi}{\partial y^2}\right) dx\, dy + \int_{s} \underline{\alpha}h\, ds \quad .$$

Expressing the above in a matrix form yields the linear system of equations

$$S_{ij}P_j = b_i + C_i \quad . \tag{4.16}$$

Before the pressure field solution can be sought the ψ nodes values that occur on the right hand-side of equation (4.14) must be known beforehand, on an element by element basis. The Gaussian quadrature integration scheme requires the integrand to be evaluated at the Gauss points of every element. The process of evaluating the second derivative at a point is outlined in Appendix A.

The no-slip pressure boundary condition can be expressed in terms of ψ, as in equation (2.15), or in terms of ω, as in equation (2.16). The third derivative of ψ must be evaluated if equation (2.15) is used. Evaluating the third derivative of a field represented by serendipity shape functions, is inherently more inaccurate than the second derivative: the higher the order the greater the inaccuracy. One could use equation (2.15), even with quadratic serendipity shape functions, but equation (2.16) is preferred.

The system matrix S_{ij} in equation (4.16) is identical to the system matrices of equations (4.4) and (4.8). The

matrix S_{ij} is positive definite and symmetric. A variety of matrix solution techniques can be applied to solve a symmetric positive definite matrix. In this study, a sparse preconditioned Cholesky conjugate gradient method was used [26, 27]. The conjugate gradient method was chosen over the Crout method because it is computationally more efficient at solving a sparse and symmetric set of linear equations.

Chapter V

SOLVED PROBLEMS AND SOME REMARKS

Presented are some two-dimensional laminar flow examples which demonstrate the versatility and accuracy of the finite element method described in this thesis. A finite element mesh generation package called MANDAP [28] was used to eliminate the time-consuming and cumbersome job of preparing the quadrilateral mesh for each flow example. A general FORTRAN IV program was written. All numerical computations are performed in real single precision. The examples were computed with an AMDAHL 470/V8 mainframe.

5.1 FLOW PAST A CIRCULAR CYLINDER

Consider the steady two-dimensional flow of an incompressible viscous fluid around a circular cylinder of radius one. The flow is assumed to possess symmetry about the x-axis, allowing the problem domain to be reduced to the upper half of the flow field. The finite element mesh shown in Figure 5.1, consists of 101 elements and 356 nodes.

The ψ boundary conditions correspond to a uniform flow of u=1.0 and v=0.0. Due to the presence of a downstream wake, the downstream portion of the mesh should be extended to infinity before uniform flow boundary conditions can be

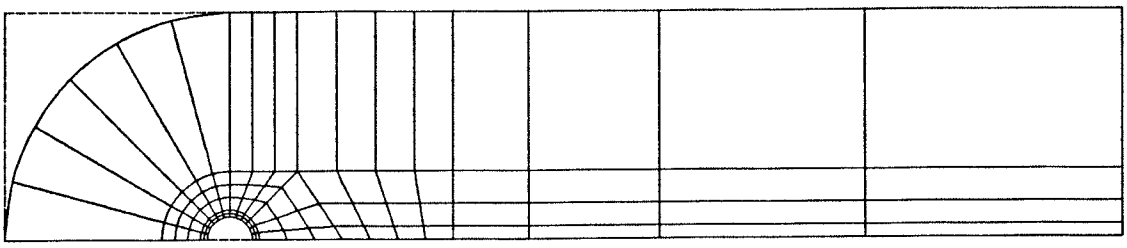

Figure 5.1: Circular cylinder finite element mesh.

applied. In this example, it is assumed that the mesh is sufficiently large, especially in the downstream portion, to allow uniform flow boundary conditions to be enforced. Extending the mesh by simply adding on more and more elements is not practical because of the larger number of elements involved. As alternatives, infinite elements [29, 30] or picture-frame methods [31] could be implemented. The implementation of such methods was not attempted in this study, but is worth further investigation.

On the circular cylinder surface the no-slip boundary conditions are applied. ω along the mesh boundaries is set to zero everywhere except along the no-slip surface. Along the no-slip surface ω remains unknown.

To be consistent with previous work, the characteristic length L_0 is taken to be the radius of the circular cylinder. Hence, for this example the Reynolds number is defined by

$$Re = \frac{2U_0 r}{\nu} \quad ,$$

where r represents the radius.

The flow around a circular cylinder was analyzed for the Reynolds numbers of 10, 50, and 100. During each Newton-Raphson iteration the potentials of 527 nodes were updated. With a zero starting estimate, an average of five to six iterations were required to satisfy the exit criterion of 0.0001. The computational time required to perform the five or six iterations was of the order of 200 to 500 seconds. Most of the computational time went into solving equation (4.10) during each iteration. A sample plot of the ψ and ω solution, for a Reynolds number of 100, are shown in Figures 5.2a and 5.2b.

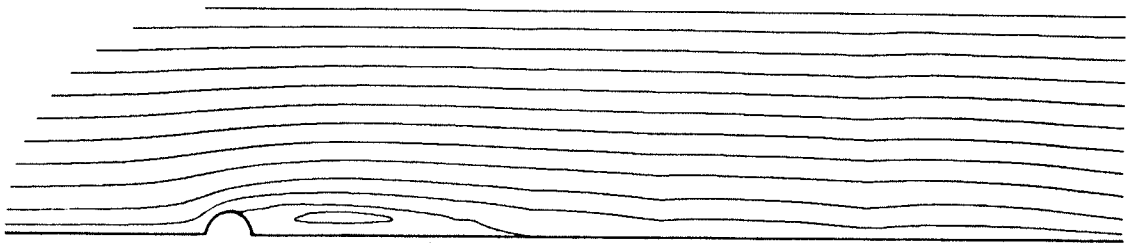

a) Stream function contours

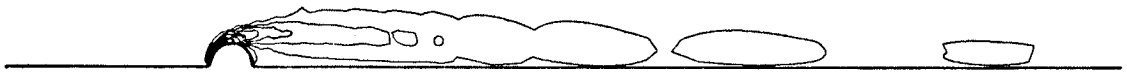

b) Vorticity contours

Figure 5.2: Circular cylinder contour plots (Re=100).

The ω values along the no-slip boundary do not form a smooth and regular contour; the node values fluctuate slightly. It was found that the node fluctuation is highly dependent upon the accuracy with which the no-slip surface is modeled. Figure 5.3 demonstrates the effect of introducting a 1% error in the node coordinates of three individual nodes that lie on the no-slip surface. The perturbed nodes were placed at a radial distance of 0.99.

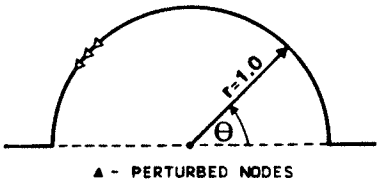

Surface representation

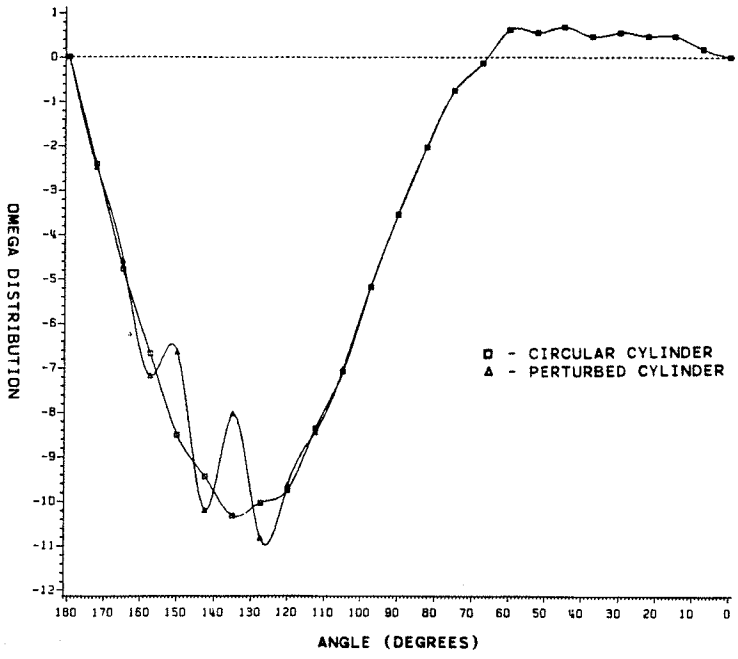

Figure 5.3: Circular cylinder node perturbation (Re=100).

A least-squares smoothing algorithm, with Legendre polynomial basis [25], is used to smooth the ω node values that lie on the no-slip boundary. Plots of the no-slip ω values for the Reynolds numbers of 10, 50 and 100 are shown in Figure 5.4. The obtained results are in good agreement with the results of Taunn & Olson [32], and Dennis & Chang [33].

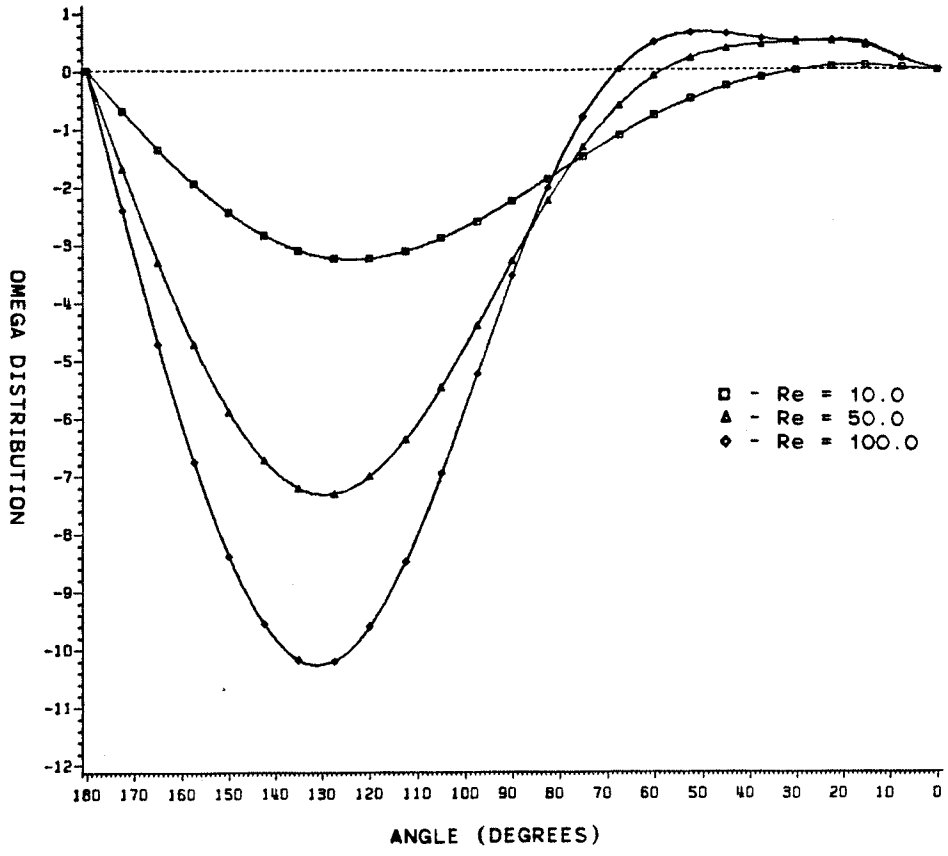

Figure 5.4: Vorticity distribution on the circular cylinder.

The Newton-Raphson iterative process was found to be very stable, exhibiting a near quadratic convergence rate for any

Reynolds number of 100 or less. Initially tests performed at a Reynolds number of 200 failed to converge. This indicated that an initial guess of zero for the node potentials is not close enough to the solution to facilitate convergence. An intermediate field solution at a Reynolds number of 100 was necessary to improve the starting estimate. Five iterations were performed at a Reynolds number of 100 and another six iterations followed at a Reynolds number of 200 before the exit criteria of 0.0001 was satisfied.

The pressure field solution utilizes the already determined ψ node values and the least-squares smoothened ω node values. Three pressure boundary conditions are applied: a) a zero Dirichlet condition along the top and both sides of the mesh; b) a natural Neumann condition along the two bottom halves and; c) the Neumann pressure equation (2.16) along the no-slip surface. For the Reynolds numbers of 10, 50 and 100, the pressure solution was determined and the pressure distribution along the circular cylinder are presented in Figure 5.5. A pressure contour plot, for a Reynolds number of 100, is shown in Figure 5.6.

The accuracy of the pressure results is directly dependent upon the accuracy with which the ψ and ω field solutions are determined. A slight error in either the ψ field or the ω field is magnified by the derivative operator. Since derivative evaluation is an essential part of the pressure field calculations, the pressure solution

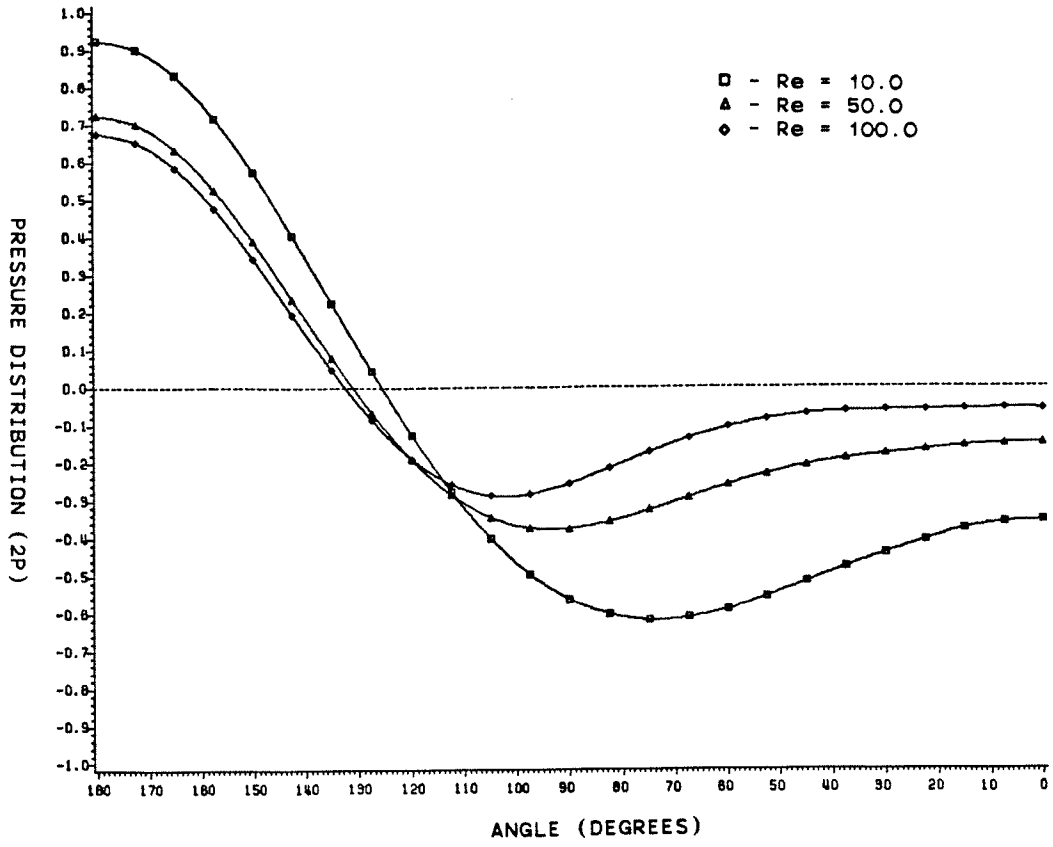

Figure 5.5: Pressure distribution on the circular cylinder.

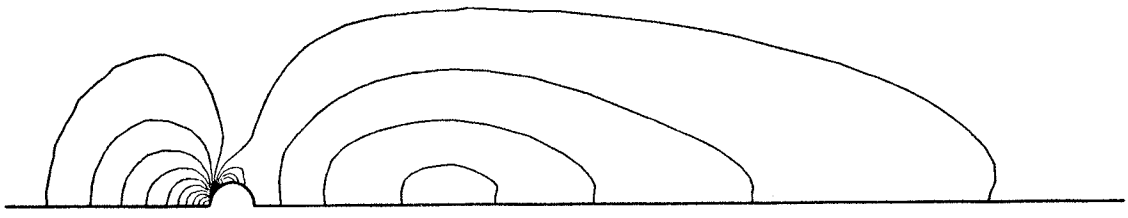

Figure 5.6: Circular cylinder pressure contours (Re=100).

will be inherently more inaccurate. This is one drawback of the ψ and ω formulation.

5.2 FLOW IN A CHANNEL WITH A STEP

The second example considered is the plane flow of a viscous fluid in a channel with a sudden expansion, the expansion ratio being 2:3. This example demonstrates the application of the finite element method to an internal flow problem.

The dimensions of the channel inlet and step height h are shown in Figure 5.7. At the inlet a fully developed parabolic velocity profile is assumed; $u=4y(1-y)$ and $v=0.0$. The inlet ψ and ω boundary conditions are described by the assumed velocity profile. The outlet ψ and ω boundary conditions are both natural Neumann. Along the channel walls the no-slip condition is applied.

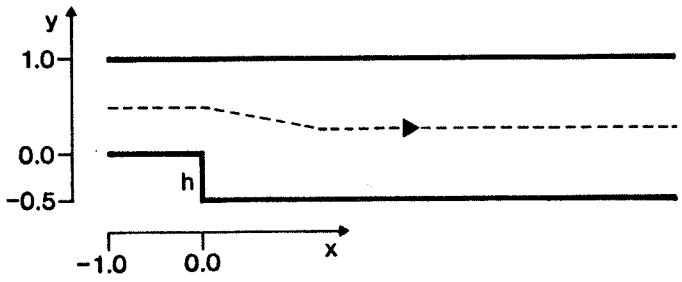

Figure 5.7: Channel inlet and step dimensions.

The finite element mesh shown in Figure 5.8, consists of 81 elements and 286 nodes. The Reynolds number for this problem is based on the step height h

$$Re = \frac{U_0 h}{\nu} \quad .$$

It was observed that for a Reynolds number less than 70, the iterative process was stable and convergence proceeds rapidly. When higher Reynolds numbers were tried, a solution at a lower Reynolds was required before the iterative process converged. The exit criterion for this problem was set to 0.0001. The ψ and ω field contours are shown in Figure 5.9a and 5.9b, respectively.

With the Reynolds number equal to 150, the computational time taken to perform the nine iterations was 380 seconds. This time could be significantly reduced if a more efficient matrix solution method was implemented to solve equation (4.10). Also, utilizing a sparsity storage scheme would dramatically reduce computer storage requirements.

Along the no-slip surface two boundary conditions are enforced, a constant Dirichlet and a natural Neumann. Inspection of the ψ results reveals that all no-slip surfaces are at an equipotential. As a check, the normal ψ derivatives on the no-slip surfaces were evaluated at several points just downstream of the step. The normal derivatives were numerically determined by taking the dot product of the normal unit vector with the ψ gradient vector. The magnitude of the derivative values were found to lie between 0.01 and 0.0001. To put these numbers into perspective, one must consider the field variation of ψ. In

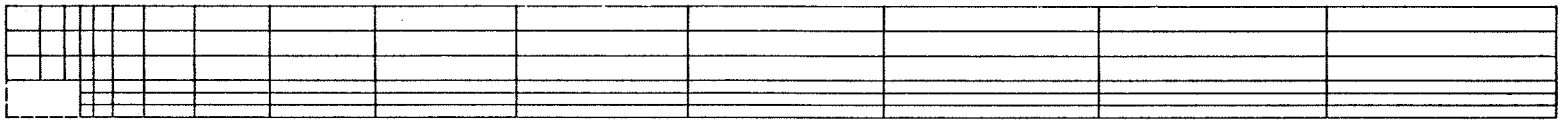

Figure 5.8: Finite element mesh for a channel with a step.

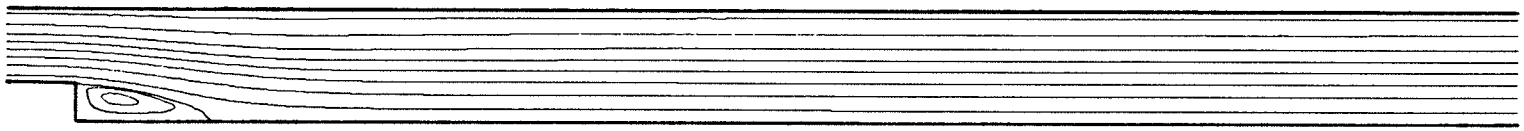

a) Stream function contours

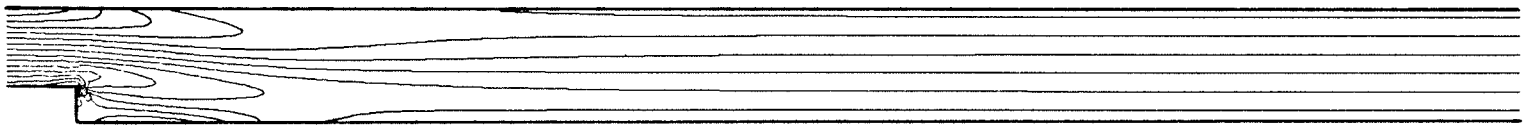

b) Vorticity contours

Figure 5.9: Channel flow contour plots for a Reynolds number of 150.

this example, the stream function values vary from -0.01 to 2/3, i.e. a derivative of the order of unity. The numerically derived derivatives, at the boundary, are at least two orders of magnitude less than the internal field variation. This indicates that a natural Neumann condition is being enforced.

In comparison with other investigations [34, 35], the ψ and ω fields are very smooth and continuous. Good convergence characteristics are exhibited for all laminar Reynolds numbers tested. The results obtained compare favorably, even with such a coarse mesh.

In this study, no attempt was made to evaluate the third-order derivative terms in equation (2.13). Because of this, the pressure solution is not available for this example.

Chapter VI

CONCLUSIONS

This thesis has shown that a direct variational finite element method is a viable and efficient solution technique for the laminar two-dimensional Navier-Stokes equations. The advantage of formulating the Navier-Stokes equations in terms of the stream function and vorticity variables is that the velocity field solution is separated from the pressure solution. In the process of separating the two fields, the number of unknowns is reduced. There are only two simultaneous unknowns ψ and ω. Both the velocity field and pressure field can be determined by post-processing the ψ and ω solution.

The applied Newton-Raphson iterative solution process exhibits acceptable convergence characteristics for a diverse range of flow problems. The number of iterations necessary to achieve convergence increase as the Reynolds number increases. In the sample problems, the process converged for all laminar Reynolds numbers tested.

A new approach to handling the no-slip condition was developed in this study. The no-slip boundary conditions are introduced directly into the Newton-Raphson Jacobian matrix by performing a set of row and column permutations.

When the constant ψ no-slip boundary condition is not known beforehand, an alternative method of introducing the no-slip conditions is required. The proposed method of enforcing an equipotential surface has practical limitations. More research is necessary before the question of how to handle the no-slip condition for unknown ψ is completely answered.

The dynamics of fluid flow make it vitally important that all no-slip surfaces be accurately modeled. Any deviation in the no-slip surface representation, whether it is a small surface indentation or a derivative inflection, induces large fluctuations of ω along the surface. A serendipity representation of a curved surface contains geometric derivative discontinuities at adjacent elements. The presence of derivative discontinuities would explain the variation of ω along the no-slip surface and the need for least-squares smoothing. The magnitude of the derivative discontinuities can be kept to a minimum by ensuring that there are a sufficient number of elements to model the surface. It is recommended that the implementation of higher order surface modelling techniques, such as splines, be investigated.

In post-processing the ψ and ω solution, to obtain the pressure field, one is required to evaluate derivatives. Depending on the problem, up to third-order derivatives may be required. When numerically evaluating a derivative it is inevitable that some accuracy will be lost. The pressure

results presented in the circular cylinder example illustrates that an accurate solution can be obtained despite this problem.

In summary, the variational finite element method solution technique developed in this thesis has demonstrated the ability to cater to a variety of laminar flow problems with computational efficiency. A direct method of introducing the no-slip boundary conditions has been presented. In analyzing the numerical results, several recommendations were made. It is suggested that the following points be considered in future work:

1. that higher-order surface modeling techniques be implemented;
2. that a generalized method of handling conditions at infinity be included in the finite element method; and
3. that an efficient, sparse matrix inversion method be found to invert the Jacobian matrix.

Appendix A

GLOBAL DERIVATIVE EVALUATION

To evaluate the derivative of a scalar field $\phi(x,y)$ we require the derivatives of the interpolating functions, that are expressed in terms of ξ and η, with respect to x and y.

$$\frac{\partial \phi}{\partial x} = \sum_{i=1}^{8} \frac{\partial \alpha_i}{\partial x} \phi_i$$

$$\frac{\partial \phi}{\partial y} = \sum_{i=1}^{8} \frac{\partial \alpha_i}{\partial y} \phi_i$$

Applying the rules of partial differentiation for the first derivative of the shape functions with respect to ξ and η yields two independent equations. These equations can be expressed in a matrix form to give

$$\begin{bmatrix} \frac{\partial \alpha_i}{\partial \xi} \\ \frac{\partial \alpha_i}{\partial \eta} \end{bmatrix} = \begin{bmatrix} \frac{\partial x}{\partial \xi} & \frac{\partial y}{\partial \xi} \\ \frac{\partial x}{\partial \eta} & \frac{\partial y}{\partial \eta} \end{bmatrix} \begin{bmatrix} \frac{\partial \alpha_i}{\partial x} \\ \frac{\partial \alpha_i}{\partial y} \end{bmatrix} = J \begin{bmatrix} \frac{\partial \alpha_i}{\partial x} \\ \frac{\partial \alpha_i}{\partial y} \end{bmatrix} . \qquad (A.1)$$

The entries of the Jacobian of transformation matrix J are easily evaluated. In order to obtain the derivatives of the interpolating functions the matrix J is inverted.

$$\begin{bmatrix} \frac{\partial \alpha_i}{\partial x} \\ \frac{\partial \alpha_i}{\partial y} \end{bmatrix} = \frac{\begin{bmatrix} \frac{\partial y}{\partial \eta} & -\frac{\partial y}{\partial \xi} \\ -\frac{\partial x}{\partial \eta} & \frac{\partial x}{\partial \xi} \end{bmatrix}}{\det[J]} \begin{bmatrix} \frac{\partial \alpha_i}{\partial \xi} \\ \frac{\partial \alpha_i}{\partial \eta} \end{bmatrix}$$

Using the first derivatives, given in (A.1), the second partial derivatives of the interpolating functions can be determined. Taking the second partial derivatives of the shape functions results in

$$\begin{bmatrix} \left(\frac{\partial x}{\partial \xi}\right)^2 & 2\frac{\partial x}{\partial \xi}\frac{\partial y}{\partial \xi} & \left(\frac{\partial y}{\partial \xi}\right)^2 \\ \frac{\partial x}{\partial \xi}\frac{\partial x}{\partial \eta} & \frac{\partial x}{\partial \xi}\frac{\partial y}{\partial \eta} + \frac{\partial x}{\partial \eta}\frac{\partial y}{\partial \xi} & \frac{\partial y}{\partial \xi}\frac{\partial y}{\partial \eta} \\ \left(\frac{\partial x}{\partial \eta}\right)^2 & 2\frac{\partial x}{\partial \eta}\frac{\partial y}{\partial \eta} & \left(\frac{\partial y}{\partial \eta}\right)^2 \end{bmatrix} \begin{bmatrix} \frac{\partial^2 \alpha_i}{\partial x^2} \\ \frac{\partial^2 \alpha_i}{\partial x \partial y} \\ \frac{\partial^2 \alpha_i}{\partial y^2} \end{bmatrix} = \begin{bmatrix} \frac{\partial^2 \alpha_i}{\partial \xi^2} - \frac{\partial \alpha_i}{\partial x}\frac{\partial^2 x}{\partial \xi^2} - \frac{\partial \alpha_i}{\partial y}\frac{\partial^2 y}{\partial \xi^2} \\ \frac{\partial^2 \alpha_i}{\partial \xi \partial \eta} - \frac{\partial \alpha_i}{\partial x}\frac{\partial^2 x}{\partial \xi \partial \eta} - \frac{\partial \alpha_i}{\partial y}\frac{\partial^2 y}{\partial \xi \partial \eta} \\ \frac{\partial^2 \alpha_i}{\partial \eta^2} - \frac{\partial \alpha_i}{\partial x}\frac{\partial^2 x}{\partial \eta^2} - \frac{\partial \alpha_i}{\partial y}\frac{\partial^2 y}{\partial \eta^2} \end{bmatrix} .$$

In evaluating the matrix entries it is necessary to determine both the first and second derivatives at a point.

Regardless of the order, the process of determining the matrix entries and inverting is repeated for all eight interpolating functions. The values are then summed appropriately to give the global derivative values at any given point within an element.

REFERENCES

1. Larock, B. E. and Schamber, D. R. 'Finite Element Computation of Turbulent Flows.', Adv. Water Resources, Vol. 4, December 1981.

2. Bradshaw, P., Cebeci, T. and Whitelaw, J. Engineering Calculation Methods for Turbulent Flow. Academic Press Inc., London, 1981.

3. Chung, T.J. Finite Element Analysis in Fluid Dynamics. McGraw-Hill Inc., New York, 1978.

4. Wu, J. C. and Thompson, J. F. 'Numerical Solutions of Time-Dependent Incompressible Navier-Stokes Equations Using an Integro-Differential Formulation.', Computers and Fluids, Vol. 1 (1973) 197-215.

5. Liggett, J. A. and Liu, P. L-F. The Boundary Integral Equation Method for Porous Media Flow. George Allen & Unwin Ltd, London, 1983.

6. Dhatt, G., Fomo, B. and Bourque, C. 'A ψ-ω Finite Element Formulation for the Navier-Stokes Equations.', International J. for Numerical Methods in Engng, Vol. 17 (1981) 199-212.

7. Campion-Renson, A. and Crochet, M. J. 'On the Stream Function-Vorticity Finite Element Solutions of Navier-Stokes Equations.', International J. for Numerical Methods in Engng, Vol. 12 (1978) 1809-1818.

8. Hughes, T. J., Liu, W. K. and Brooks, A. 'Finite Element Analysis of Incompressible Viscous Flows by the Penalty Function Formulation.', J. of Computational Physics, Vol. 30 (1979) 1-60.

9. Schlichting, H. Boundary-Layer Theory. Sixth Edition, McGraw-Hill Inc., New York, 1968.

10. Roache, P.J. Computational Fluid Dynamics. Second Edition, Hermosa Publishers, Albuquerque, New Mexico, 1976.

11. Pearson, C.E. 'A Computational Method for Viscous Flow Problems.', J. Fluid Mech., Vol. 21 (1965) 611-622.

12. Tottenham, H. 'Direct Variational Techniques.', Variational Methods in Engineering. Southampton University Press, Vol. 1, 1973.

13. Mikhlin, S.G. Variational Methods in Mathematical Physics. Pergamon Press Ltd, New York, 1964.

14. Wexler, A. Finite Elements For Technologists. Tech. Rept. TR 80-4, Dept. of Elec. Engng, University of Manitoba, Canada, 1980.

15. Zienkiewicz, O.C. The Finite Element Method. Third Edition, McGraw-Hill Inc., London, 1977.

16. Stroud, A.H. and Secrest, D. Gaussian Quadrature Formulas. Prentice-Hall Inc., Englewood Cliffs, N. J., 1966.

17. Ascher, U., Pruess, S. and Russell, R. 'On Spline Basis Selection for Solving Differential Equations.', SIAM J. Numer. Anal., Vol. 20, No. 1, February 1983.

18. Bathe, K.J. and Cimento, A.P. 'Some Practical Procedures for the Solution of Nonlinear Finite Element Equations.', Computer Methods in App. Mech. and Engng, Vol. 22 (1980) 59-85.

19. Bellman, R. Methods of Nonlinear Analysis. Academic Press, New York, Vols. 1,2 and 3, 1970.

20. Saaty, T.L. and Bram, J. Nonlinear Mathematics. McGraw-Hill Inc., New York, 1964.

21. Taylor, C. and Hood, P. 'A Numerical Solution of the Navier-Stokes Equations Using the Finite Element Technique.', Computers and Fluids, Vol. 1 (1973) 73-100.

22. Wu, J.C. 'Theory for Aerodynamic Force and Moment in Viscous Flows.', AIAA Journal, Vol. 19, No. 4, April 1981.

23. Karamcheti, K. Principles of Ideal-Fluid Aerodynamics John Wiley and Sons Inc., New York, 1966.

24. Tewarson, R.P. Sparse Matrices. Academic Press Inc., New York, 1973.

25. International Mathematical and Statistical Libraries, Inc. The IMSL Library, Reference Manual. Houston, Texas, USA, Vol. 2, 1982.

26. Nakonechny, R.L. 'A Preconditioned Conjugate Gradient Method Using a Sparse Linked-list Technique for the Solution of Field Problems.', M.Sc. Dissertation, Dept. of Elec. Engng, University of Manitoba, Canada, May 1983.

27. Kershaw, D.S. 'The Incomplete Cholesky-Conjugate Gradient Method for the Iterative Solution of Systems of Linear Equations.', J. of Computational Physics, Vol. 26 (1978) 43-65.

28. Yildir, Y.B. and Wexler, A. MANDAP a Finite Element Method/Boundary Element Method Data Preparation Package - User's Manual. Tech. Rept. TR82-3, Dept. of Elec. Engng, University of Manitoba, Canada, 1982.

29. Bettess, P. 'More on Infinite Elements.', International J. for Numerical Methods in Engng, Vol. 15 (1980) 1613-1626.

30. Pissanetzky, S. 'An Infinite Element and a Formula for Numerical Quadrature Over an Infinite Interval.', International J. for Numerical Methods in Engng, Vol. 19 (1983) 913-927.

31. McDonald, B.H. and Wexler, A. 'Mutually Constrained Partial Differential and Integral Equation Field Formulations.', Finite Elements in Electrical and Magnetic Field Problems. John Wiley & Sons Ltd, 1980, 161-190.

32. Tuann, S. and Olson, M.D. 'Numerical Studies of the Flow Around a Circular Cylinder by a Finite Element Method.', Computers and Fluids, Vol. 6 (1978) 219-240.

33. Dennis, S.C.R. and Chang, G. 'Numerical Solutions for Steady Flow Past a Circular Cylinder at Reynolds Numbers up to 100.', J. Fluid Mech., Vol. 42, part 3, (1970) 471-489.

34. Thomas, C.E., Morgan, K. and Taylor, C. 'A Finite Element Analysis of Flow Over a Backward Facing Step.', Computers and Fluids, Vol. 9 (1981) 265-278.

35. Atkins, D.J., Maskell, S.J. and Patrick, M.A. 'Numerical Prediction of Separated Flows.', International J. for Numerical Methods in Engng, Vol. 15 (1980) 129-144.